Supplementary Figure 1

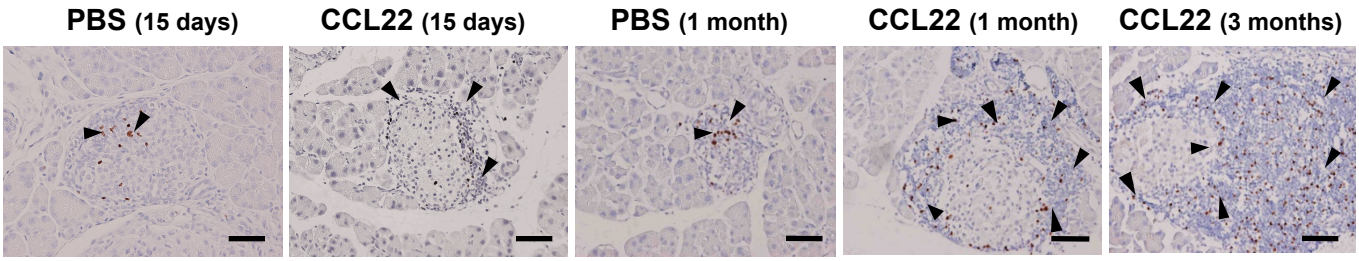

Supplementary Figure 1. Detection of Foxp3^{+} cells in pancreas.

Immunostaining of pancreas sections showing Foxp3^{+} cells surrounding the islet (arrows). Scale bar=100 μm for all images.

Supplementary Figure 2

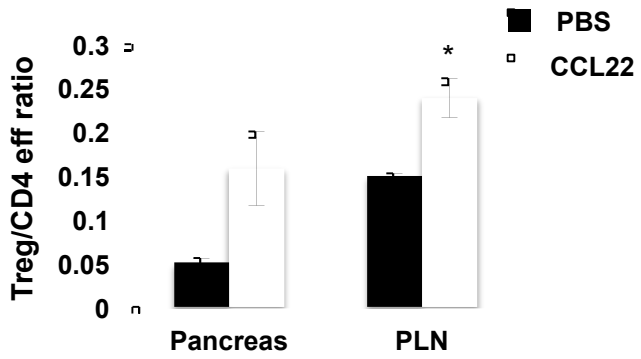

Supplementary Figure 2. Treg/CD4 effector ratios are increased in CCL22-NOD mice.

The ratio of Tregs ($CD4^+Foxp3^+$) to CD4eff ($CD4^+$ $FoxP3^-$) was determined in the pancreas and PLN at one month after injection by flow cytometry for PBS control (N=4) and CCL22-NOD (N=5). CCL22-NOD vs PBS-NOD *p*=NS in pancreas and *p=0.02 in PLN.

Supplementary Figure 3

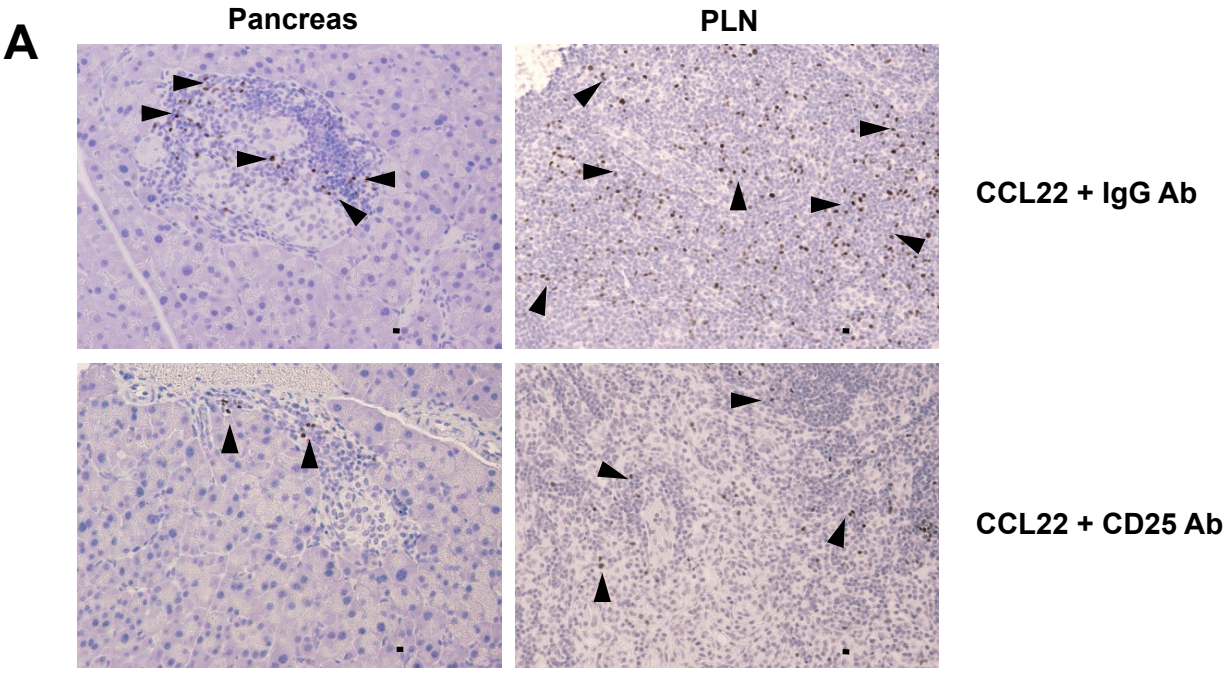

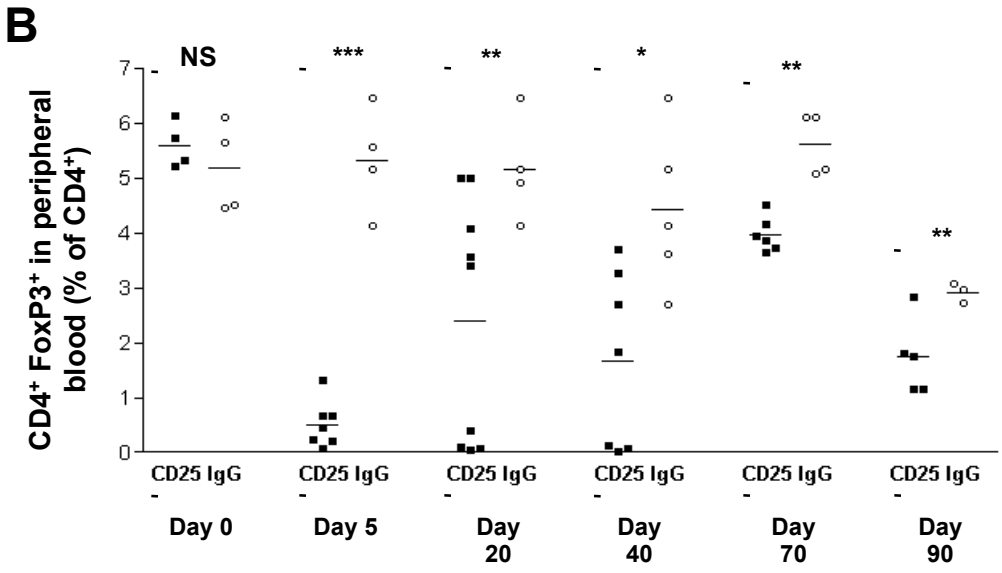

Supplementary Figure 3. CD25 Ab depletes Tregs in CCL22-NOD mice

(A) Histological analysis of pancreas and PLN from CCL22-NOD mice treated with IgG or anti-CD25 antibody. Immunostaining showing that Foxp3$^+$ cells (arrows) are decreased in tissues of mice treated with anti-CD25 antibody. A representative animal is shown. Scale bar = 100μm for all images. **(B)** Flow cytometric analysis of CD4$^+$FoxP3$^+$ cells in blood of CCL22-NOD mice treated with anti-CD25 (■) or isotype-matched control IgG (o).***p<0.001, **p<0.01, *p<0.05. Line between squares indicates mean.

Supplementary Figure 4

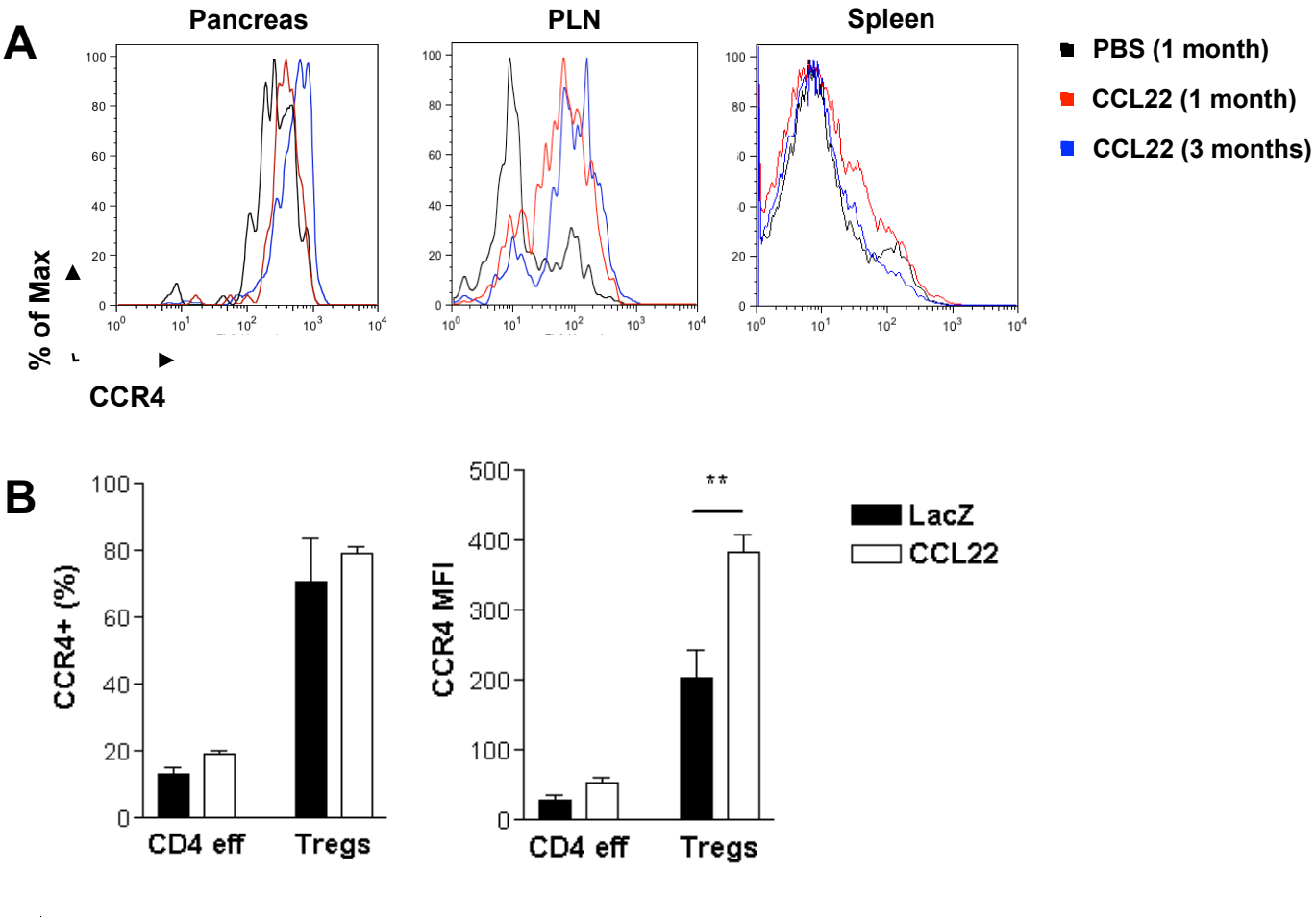

Supplementary Figure 4. CCR4 expression is increased in CCL22-expressing mice.

(A) CCR4 expression on Tregs in pancreas, PLN and spleen of CCL22-NOD at 1 and 3 months after injection. Cells in the $CD4^{+}Foxp3^{+}$ gate were analyzed for expression of CCR4. N=2 for each group (p=NS). A representative animal is shown. **(B)** CCR4 expression on $CD4^{+}$ $FoxP3^{-}$ effector T cells and $CD4^{+}$ $FoxP3^{+}$ Tregs in CCL22- (n=4) and LacZ-expressing grafts (n=3) 10 days post-transplant, determined by flow cytometry. Left panel: CCR4+ cells as percent of CD4 effector cells or Tregs. *p*=NS. Right panel: Tregs in CCL22 grafts express higher levels of CCR4 than in LacZ grafts. Data shown as mean fluorescence intensity (MFI) of CCR4 in indicated cell populations. ***p*=0.01 vs LacZ.

Supplementary Figure 5

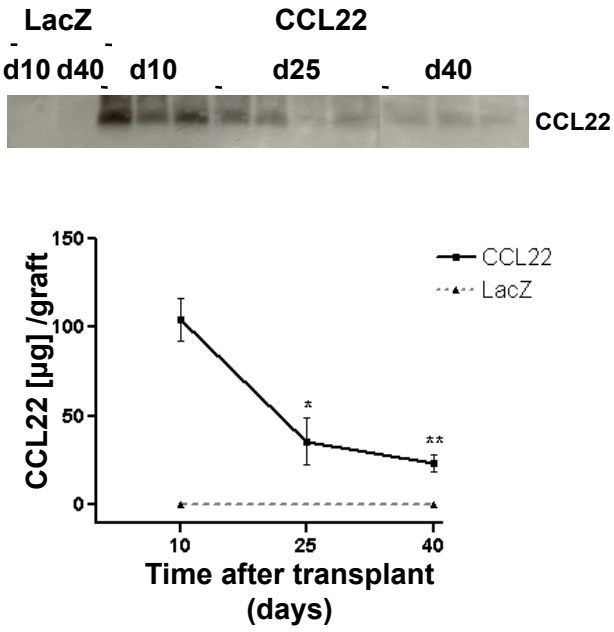

Supplementary Figure 5. CCL22 expression decays with in syngeneic islet grafts.

CCL22 levels determined by Western blot (upper panel) and ELISA (lower panel) in Ad-CCL22 or Ad-LacZ transduced NOD.*scid* islets transplanted into STZ-diabetic NOD.*scid* recipients and harvested at indicated times post-transplantation. Results are expressed as mean ± SEM. *p<0.05 and **p<0.01 *vs* CCL22 at day 10.

Supplementary Figure 6

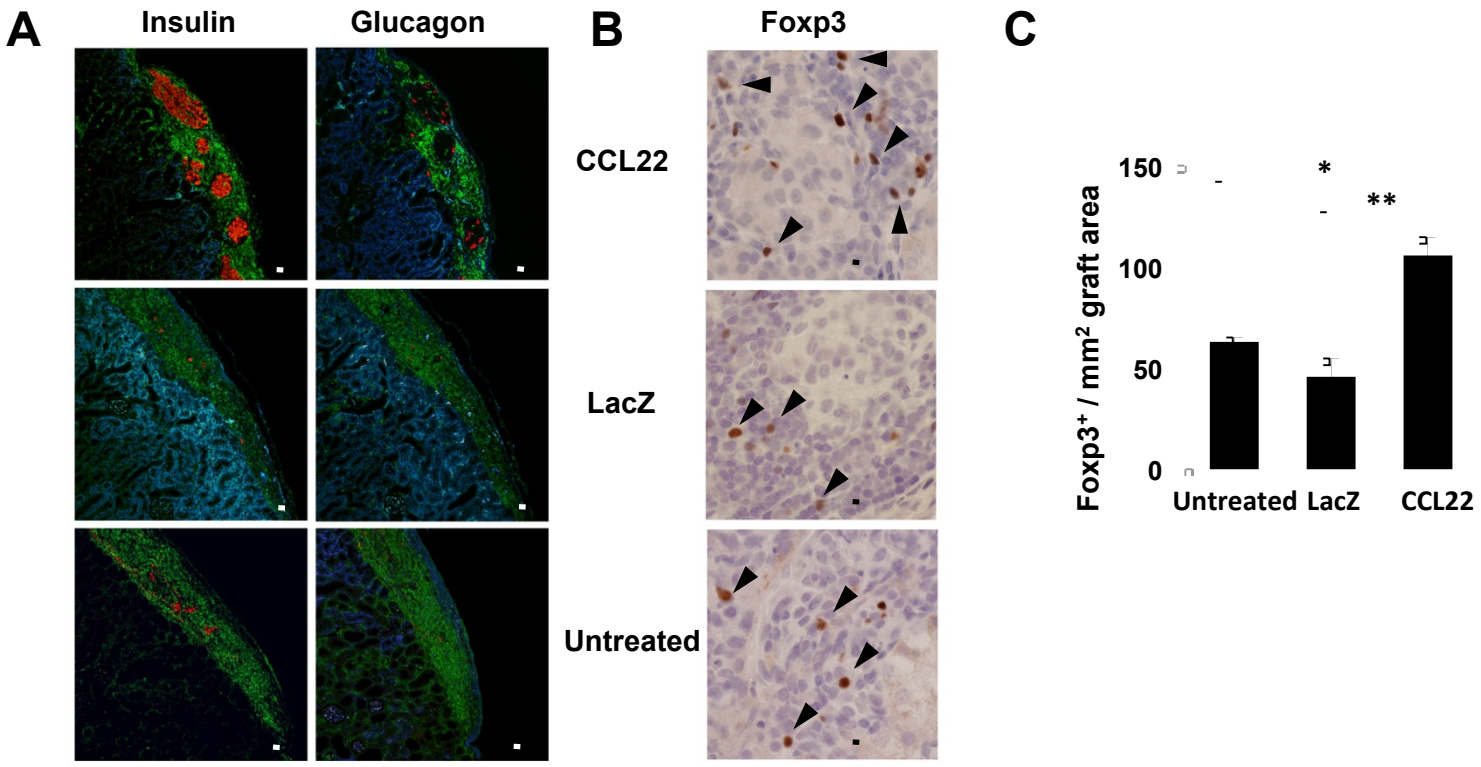

Supplementary Figure 6. Histological analysis of islet grafts.

(A) Immunostaining of sections of islet grafts 10 days post-transplantation for insulin- or glucagon-positive cells (red), and $CD45^+$ cells (green). Pictures shown are representative of grafts examined from mice of each treatment group. **(B)** Sections of the same grafts immunostained for $FoxP3^+$ cells (arrows) showing presence of increased proportion of $Foxp3^+$ cells in CCL22-expressing grafts. Scale bar = 100 µm for all images. **(C)** Treg numbers were determined as a proportion of infiltrated graft area on sections immunostained for FoxP3. One representative section from each graft was analyzed (CCL22: n=4; LacZ: n=3; control: n=2). *p<0.05 and **p<0.01.

Supplementary Figure 7

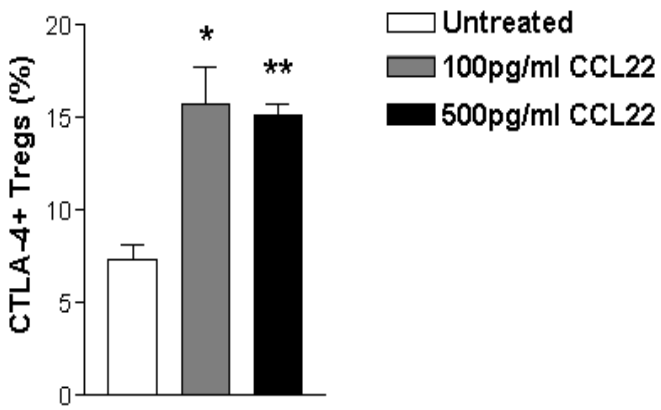

Supplementary Figure 7. CCL22 increases CTLA-4 expression on Tregs in vitro. Expression of CTLA-4 on Tregs is upregulated after 24 hours *in vitro* incubation with 100 and 500 pg/ml of recombinant mouse CCL22, as determined by flow cytometry. There was no difference in cell survival between the 3 groups during the assay. Data are representative of 3 experiments. *$p<0.05$ and **$p<0.01$ *vs* untreated.